

# Synthesis and Optical, Photoconductivity Study of Safranin O Dye Sensitized Titania/Silica oxide system Prepared by Modified Sol-gel Method

D. Arun Kumar, J. Merline Shyla, Francis P. Xavier

**Abstract:** Binary  $TiO_2/SiO_2$  oxides were prepared by modified sol-gel method and calcined at  $500^\circ C$  for 5 hours. The  $TiO_2/SiO_2$  nanocomposites was sensitized with different concentrations of Safranin O dye solutions ranging from  $1 \times 10^{-2}$  mM to  $5 \times 10^{-2}$  mM. The amount of dye adsorbed, amount of dye absorbed per unit mass and percentage of dye adsorbed increases with increase of concentration of dye. The Safranin O dye-sensitized  $TiO_2/SiO_2$  nanocomposites exhibit an intense peak at 520 nm due to  $n \rightarrow \pi^*$  transition enhances the spectral response of  $TiO_2/SiO_2$  nanocomposites to visible light. The field dependent dark and photoconductivity studies reveals that the dark and photocurrent are increase linearly with applied field. From the photoconductivity results, it was observed from the plots that for the highest concentration of dye sensitized ( $5 \times 10^{-5}$  M), the photo current density increases by an order of 75 in comparison with that of  $TiO_2/SiO_2$  nanocomposites.

**Keywords:**  $TiO_2-SiO_2$ , Oxides, Composites, Mesoporous, Photoconductivity, Semiconductors, Dye Sensitization.

## I. INTRODUCTION

Due to the non-toxicity, availability, nature and low cost,  $TiO_2$  has been the most preferred semiconductor material for the working electrode of dye sensitized solar cells. For dye-sensitized solar cells in addition to  $TiO_2$ , semiconductor used in porous nanostructured electrode includes ZnO, CdSe, CdS,  $SiO_2$ ,  $WO_3$ ,  $SnO_2$ ,  $Nb_2O_5$  and  $Ta_2O_5$  [1]. However, titanium dioxide is the most promising semiconductor for dye-sensitized nanostructured electrode for DSSCs [1]. The working electrode absorbs dye molecules and conducts photoelectrons [1]. The desirable properties of the working electrode are large surface area to absorb large amounts of dye. In order to increase the surface area, mesoporosity and to address the issue of oxygen deficiency of  $TiO_2$ ,  $SiO_2$  is added into  $TiO_2$ . At low contents of titanium oxide, titanium atoms are mainly located in tetrahedral positions of the silica network with a high dispersion, avoiding the formation of Ti-O-Ti bonds [2]. These materials show a high activity as redox catalysts, especially in epoxidation processes [3, 4]. To achieve a high light-to-energy conversion efficiency in the DSSC, dye should possess good adsorption onto the

$TiO_2$  surface and efficient electron injection into the conduction band of the  $TiO_2$  [5, 6]. The adsorption of the dye to the  $TiO_2$  surface Usually takes place through special anchoring group attached to the dye molecule. In the Safranin O dye,  $N^+Cl^-$  group will form a bond with the metal oxide surface by offering a proton to the metal oxide lattice [7]. In the present work we have synthesized  $TiO_2/SiO_2$  nanocomposites in suitable proportions by modified sol-gel method. The present work aims at studying the optical and dark and photoconductivity response of Safranin O sensitized  $TiO_2/SiO_2$  nanocomposites.

### A. Preparation of $TiO_2/SiO_2$ Nanocomposites

The solution of titanium (IV) isopropoxide  $Ti(OC_3H_7)_4$  and tetra-ethylorthosilicate  $Si(OC_2H_5)_4$  was added drop wise in isopropyl alcohol and stirred. The resultant precipitate was washed several times in alcohol and calcinated at  $500^\circ C$  for 5 hours [8].

### B. Dye sensitization of $TiO_2/SiO_2$ nanocomposites

The different concentrations of Safranin O dye solutions ranging from  $1 \times 10^{-2}$  mM to  $5 \times 10^{-2}$  mM in isopropyl alcohol were prepared. The as-synthesised  $TiO_2/SiO_2$  nanocomposites were then soaked into the dye solution for 24h until the dye molecules got completely adsorbed onto the pores of the composites [9].

### C. Characterization

The UV-Vis spectra for the synthesized samples were recorded using UV-Vis-NIR spectrophotometer at room temperature in the range 200-1000 nm. The field dependent dark and photoconductivity studies were obtained using Keithley picoammeter. The experimental setup was discussed elsewhere by Ponniah and Xavier [10].

### D. Results and Discussion

The adsorption of Safranin O dye onto the nanocomposites were carried out in a batch process by using aqueous solution of Safranin O dye in the concentration range from  $1 \times 10^{-2}$  mM to  $5 \times 10^{-2}$  mM [11]. Fig. 1 showed the UV-Vis absorption spectrum of Safranin O dye solution with different concentrations. Fig. 2 showed the calibration curve of Safranin O with different concentrations drawn from fig. 1. It clearly showed that the absorbance of the safranin O dye increases linearly with the increase of concentration of the dye solution. The concentrations of the dye solution before and after the addition of nanocomposites were calculated with the help of prepared calibration curve with standard Safranin O dye solution.

Manuscript published on 30 November 2018.

\*Correspondence Author(s)

D. Arun Kumar, Department of Physics, Bannari Amman Institute of Technology (Autonomous), Sathyamangalam, Tamil Nadu, India

J. Merline Shyla, Department of Physics, Loyola Institute of Frontier Energy (LIFE) Loyola College, Chennai, Tamil Nadu, India

Francis P. Xavier, Department of Physics, Loyola Institute of Frontier Energy (LIFE) Loyola College, Chennai, Tamil Nadu, India

© The Authors. Published by Blue Eyes Intelligence Engineering and Sciences Publication (BEIESP). This is an open access article under the CC-BY-NC-ND license <http://creativecommons.org/licenses/by-nc-nd/4.0/>



# Synthesis and Optical, Photoconductivity Study of Safranin O Dye Sensitized Titania/Silica oxide system Prepared by Modified Sol-gel Method

The amount of dye adsorbed, amount of dye adsorbed per unit mass and percentage of dye adsorbed were calculated using the

Concentration (M)	Initial Amount of dye present (mg)	Amount of dye Adsorbed (mg)	Amount of dye adsorbed in per unit mass (ppm)	% of dye adsorbed (%)
$1 \times 10^{-5}$	0.175	0.154	1.56	88.1
$2 \times 10^{-5}$	0.350	0.321	3.22	91.7
$3 \times 10^{-5}$	0.526	0.494	4.94	93.8
$4 \times 10^{-5}$	0.701	0.662	6.62	94.4
$5 \times 10^{-5}$	0.877	0.844	8.44	96.3

Table 1 Calculated values of amount of dye adsorbed per unit mass and % of dye adsorbed for different concentrations

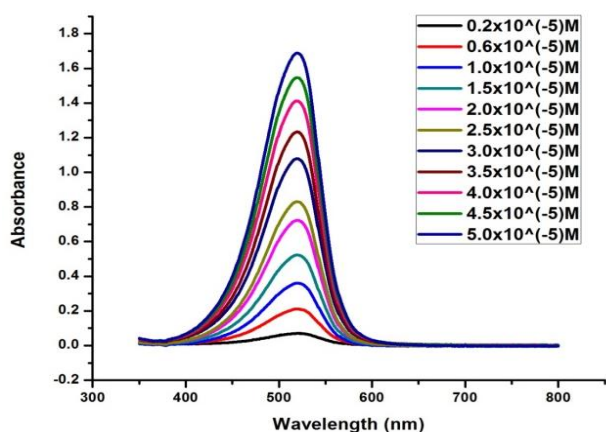


Fig. 1 UV-Vis absorption spectra of Safranin O with different concentrations

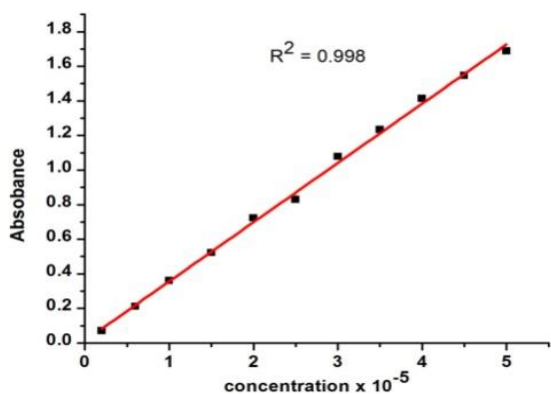


Fig. 2 Calibration curve of Safranin O with different concentrations

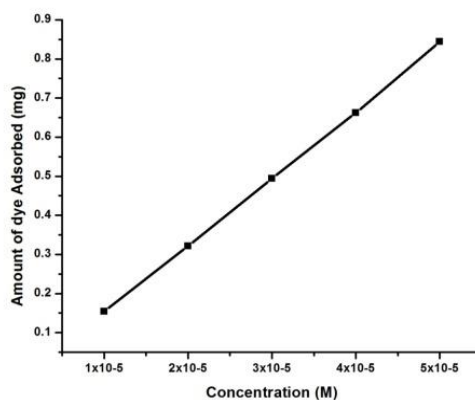


Fig. 3 Effect of concentration

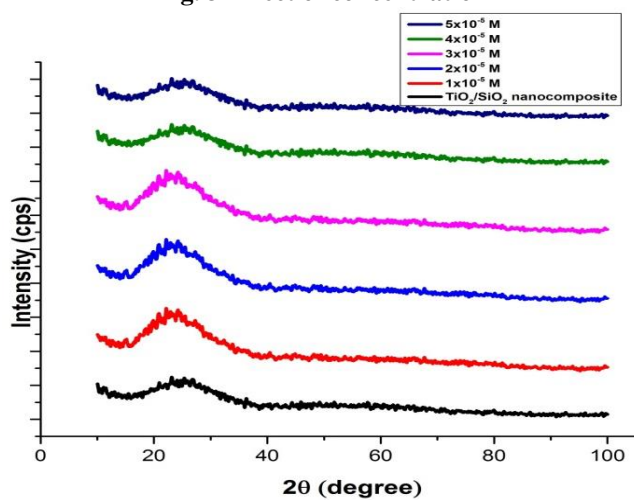


Fig. 4 XRD pattern of as-synthesized and Safranin O dye-sensitized  $\text{TiO}_2/\text{SiO}_2$  nanocomposites with different concentrations

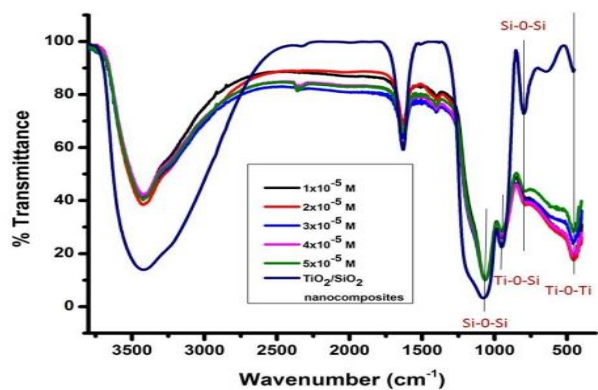


Fig. 5 Fourier Transform Infrared spectrum of pure and Safranin O dye-sensitized  $\text{TiO}_2/\text{SiO}_2$  nanocomposites with different concentrations

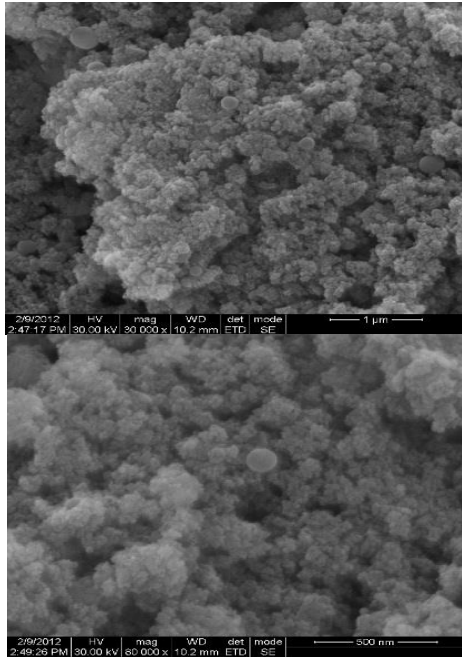


Fig. 6 HRSEM images of as-synthesized TiO<sub>2</sub>/SiO<sub>2</sub> nanocomposites

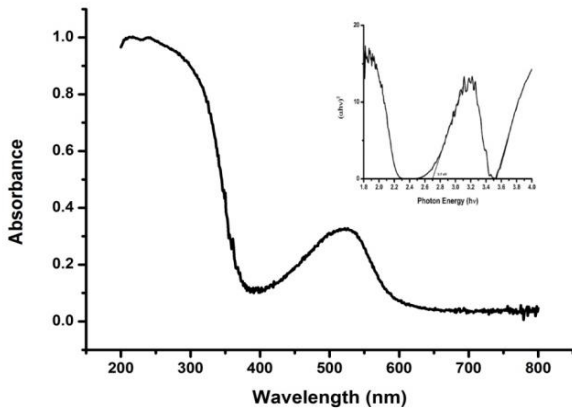


Fig. 7 UV-Vis spectrum of 1x10<sup>-5</sup> M Safranin O dye-sensitized TiO<sub>2</sub>/SiO<sub>2</sub> nanocomposites inset shows the corresponding plot of  $(\alpha h\nu)^2$  vs  $h\nu$

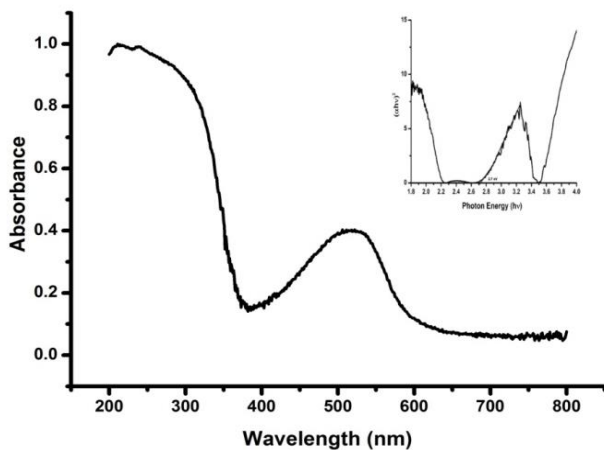


Fig. 8 UV-Vis spectrum of 2x10<sup>-5</sup> M Safranin O dye-sensitized TiO<sub>2</sub>/SiO<sub>2</sub> nanocomposites inset shows the corresponding plot of  $(\alpha h\nu)^2$  vs  $h\nu$

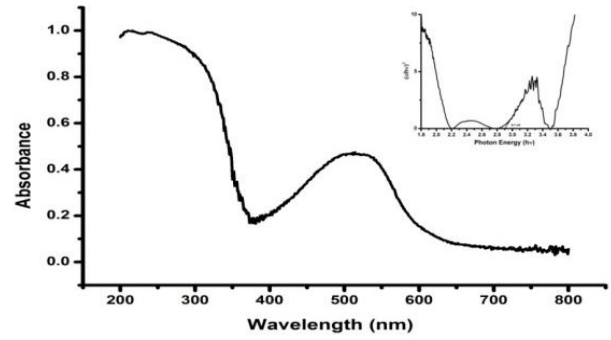


Fig. 9 UV-Vis spectrum of 3x10<sup>-5</sup> M Safranin O dye-sensitized TiO<sub>2</sub>/SiO<sub>2</sub> nanocomposites inset shows the corresponding plot of  $(\alpha h\nu)^2$  vs  $h\nu$

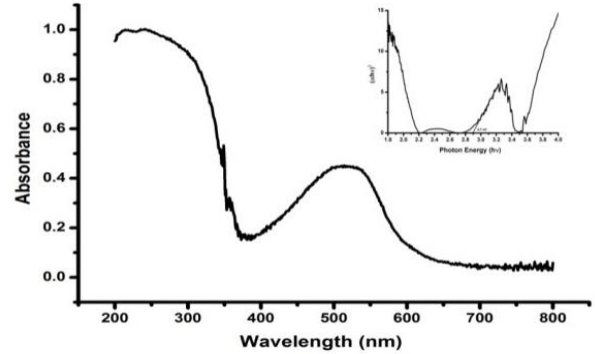


Fig. 10 UV-Vis spectrum of 4x10<sup>-5</sup> M Safranin O dye-sensitized TiO<sub>2</sub>/SiO<sub>2</sub> nanocomposites inset shows the corresponding plot of  $(\alpha h\nu)^2$  vs  $h\nu$

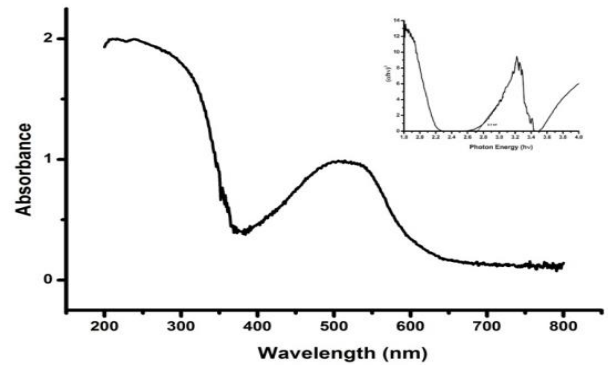


Fig. 11 UV-Vis spectrum of 5x10<sup>-5</sup> M Safranin O dye-sensitized TiO<sub>2</sub>/SiO<sub>2</sub> nanocomposites inset shows the corresponding plot  $(\alpha h\nu)^2$  vs  $h\nu$

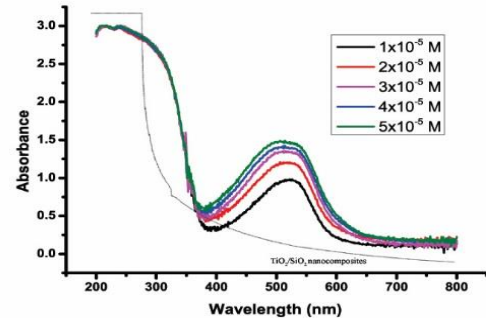


Fig. 12 UV-Vis absorption spectra of pure and Safranin O dye-sensitized TiO<sub>2</sub>/SiO<sub>2</sub> nanocomposites with different Concentrations

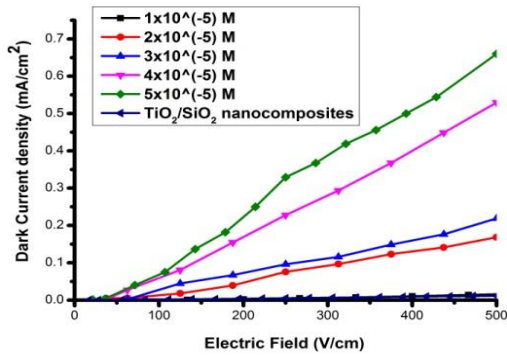


Fig. 13 Field dependent dark conductivity of Safranin O dye-sensitized TiO<sub>2</sub>/SiO<sub>2</sub> nanocomposites

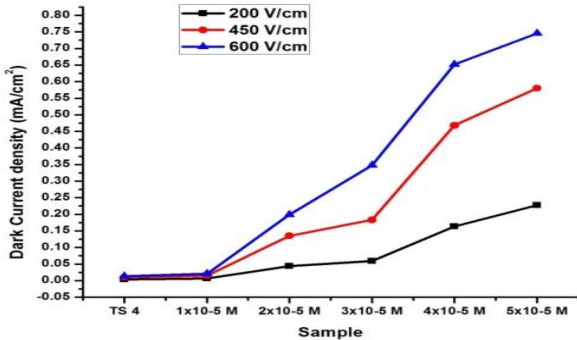


Fig. 14 Variation of dark conductivity of Safranin O dye-sensitized TiO<sub>2</sub>/SiO<sub>2</sub> nanocomposites with various fixed applied fields

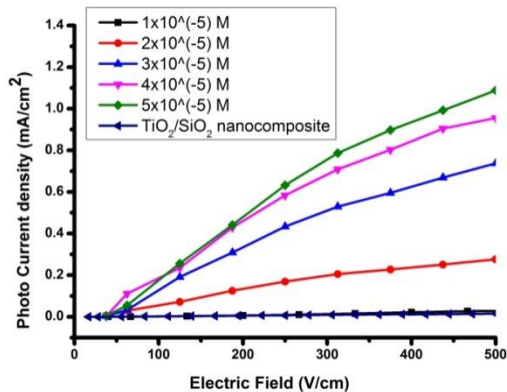


Fig. 15 Field dependent photo conductivity of Safranin O dye-sensitized TiO<sub>2</sub>/SiO<sub>2</sub> nanocomposites

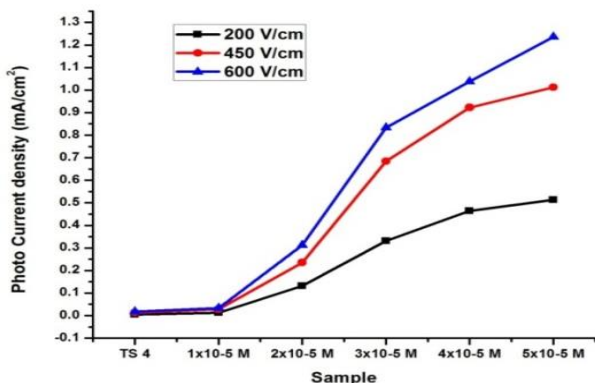


Fig. 16 Variation of photo conductivity of Safranin O dye-sensitized TiO<sub>2</sub>/SiO<sub>2</sub> nanocomposites with various fixed applied fields

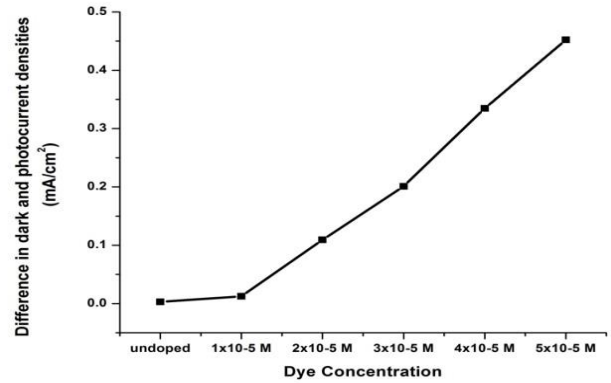


Fig. 17 Difference in dark and photo current densities vs dye concentration

Equations 1, 2, and 3 [11, 12] respectively and tabulated in table 1. It was observed that the amount of dye adsorbed, amount of dye absorbed per unit mass and Percentage of dye adsorbed increases with increase of concentration of dye.

$$\text{Amount of dye adsorbed} = (C_0 - C_e)V \quad (1)$$

$$\text{Amount of dye adsorbed per unit mass } q_e = (C_0 - C_e)V/W \quad (2)$$

$$\text{Percentage of dye adsorbed} = (C_0 - C_e)/C_0 \times 100 \quad (3)$$

Where  $q_e$ , the amount of dye adsorbed on the absorbent (mg/g).

$C_0$  and  $C_e$  (mg/L), initial and final concentration of dye solution respectively.

$V$ , volume of the dye solution (mL).

$W$ , amount of the absorbent (g).

The amount of dye adsorbed vs concentration of dye solution plot were shown in fig 3. It showed that the amount of dye adsorbed increases linearly with the increase of concentration. XRD pattern of as-synthesized and Safranin O dye-sensitized TiO<sub>2</sub>/SiO<sub>2</sub> nanocomposites with different Concentrations were shown in Fig. 4. It showed the presence of a very broad peak at 22°. The broad peak indicates that the particles are amorphous in nature [13]. The XRD results agreed with the literature that TiO<sub>2</sub> were precipitate out from the TiO<sub>2</sub>/SiO<sub>2</sub> composite because the 4-fold co-ordination of Ti will transform to 6-fold coordination upon annealing [14, 15]. This confirmed that both the TiO<sub>2</sub> and SiO<sub>2</sub> nanostructures were present. The diffraction data revealed the presence of prominent peaks due to TiO<sub>2</sub>/SiO<sub>2</sub> nanocomposites and complete absence of peaks due to Safranin O dye. The reason for the absence of peaks was due to the low concentration of dye used for sensitization and also the dye was physically adsorbed into the pores of the nanocomposites. This clearly showed that the dye was not chemically bonded to TiO<sub>2</sub>/SiO<sub>2</sub> nanocomposites.

Fourier Transform Infrared spectrum of TiO<sub>2</sub>/SiO<sub>2</sub> nanocomposites and Safranin O dye-sensitized TiO<sub>2</sub>/SiO<sub>2</sub> nanocomposites with different concentrations was shown in Fig. 5. The absorption bands at 3640 cm<sup>-1</sup> and 1630 cm<sup>-1</sup> were due to O-H stretching and bending vibrations observed in all the cases [16]. The peaks at 630 cm<sup>-1</sup>, 1110 cm<sup>-1</sup> and

800  $\text{cm}^{-1}$  corresponds to the characteristic vibrational mode for  $\text{TiO}_2$ , asymmetric and symmetric  $\text{SiO}_2$  stretching vibrations respectively [17, 18, 19, 20]. This confirmed that both  $\text{TiO}_2$  and  $\text{SiO}_2$  phases had formed in all the cases. The band near 940  $\text{cm}^{-1}$  was assigned to Ti-O-Si stretching vibration and there was complete absence of peaks due to Safranin O dye. The reason for the absence of peaks was due to the low concentration of dye used for sensitization and also the dye was physically adsorbed into the pores of the nanocomposites [21]. The dye was not chemically bonded to nanocomposites. This result coincides with the results of XRD. Thus the spectra indicated that there was physical adsorption between the nanocomposites and dye. This type of interaction may play a significant role in the photochemical reaction involving both the dye and the  $\text{TiO}_2/\text{SiO}_2$  nanocomposites. This may also influence the photosensitization, photoredox and photoexcitation processes [22]. As these compounds were used for photoconductivity and solid state electrical conductivity studies, the influence regarding such physical interactions was most valid and an important requirement.

The HRSEM images of  $\text{TiO}_2/\text{SiO}_2$  nanocomposites was shown in fig. 6. High amount of porosity was visible and also confirmed the presence of mesopores. It was observed that  $\text{TiO}_2/\text{SiO}_2$  nanocomposites were agglomerated. The particle size for synthesized  $\text{TiO}_2/\text{SiO}_2$  nanocomposite was in the range of 11 nm to 12 nm.

The UV-Vis spectrum of  $1 \times 10^{-5}$  M,  $2 \times 10^{-5}$  M,  $3 \times 10^{-5}$  M,  $4 \times 10^{-5}$  M and  $5 \times 10^{-5}$  M Safranin O dye-sensitized

$\text{TiO}_2/\text{SiO}_2$  nanocomposites and corresponding  $(\alpha h\nu)^2$  vs  $h\nu$  plot were shown in fig. 7, 8, 9, 10 and 11 respectively. Using Tauc's plot the optical band gaps of the Safranin O dye-sensitized  $\text{TiO}_2/\text{SiO}_2$  nanocomposites were calculated to be 2.7 eV and 3.5 eV. The UV-Vis absorption spectrum of as synthesized and Safranin O dye-sensitized  $\text{TiO}_2/\text{SiO}_2$  nanocomposites with different concentrations was shown in Fig.12. The Safranin O dye-sensitized  $\text{TiO}_2/\text{SiO}_2$  nanocomposites exhibited an intense peak at 520 nm due to  $n \rightarrow \pi^*$  transition [23]. On analyzing the absorption spectra of dye-sensitized  $\text{TiO}_2/\text{SiO}_2$  nanocomposites, the sensitization of nanocomposites by dye molecules in all the cases were confirmed, thereby enhancing the spectral response of  $\text{TiO}_2/\text{SiO}_2$  nanocomposites to visible light, which was further established by photoconductivity results. The dark conductivity plots of as synthesized and  $1 \times 10^{-5}$  M,  $2 \times 10^{-5}$  M,  $3 \times 10^{-5}$  M,  $4 \times 10^{-5}$  M,  $5 \times 10^{-5}$  M Safranin O dye-sensitized  $\text{TiO}_2/\text{SiO}_2$  nanocomposites with applied electric field was shown in fig. 13. All the plots indicates the linear increase of dark and photo current densities with increase in applied field depicted the ohmic nature of the contacts [16, 24, 25]. From the graph, it is evident that the dark current density values of the Safranin O dye-sensitized  $\text{TiO}_2/\text{SiO}_2$  nanocomposites increases with increase of dye concentration. Fig. 14 showed the variation of dark current density with dye concentration in Safranin O dye-sensitized  $\text{TiO}_2/\text{SiO}_2$  nanocomposites for the fixed field of 200V/cm, 450V/cm and 600V/cm. It was observed from the plots that for the highest concentration of dye ( $5 \times 10^{-5}$  M), the dark current density increased in an order of 56 in comparison

with  $\text{TiO}_2/\text{SiO}_2$  nanocomposites. For example, for a fixed field of 450V/cm, the dark current density value of as-synthesized  $\text{TiO}_2/\text{SiO}_2$  nanocomposites was 0.0104 mA, whereas the dark current value of  $5 \times 10^{-5}$  M Safranin O dye-sensitized  $\text{TiO}_2/\text{SiO}_2$  nanocomposites was 0.58 mA. The significant increase in the dark current density value of Safranin O dye-sensitized  $\text{TiO}_2/\text{SiO}_2$  nanocomposites was attributed to the enhancement of number of free charge carriers upon addition of the organic dye Safranin O to the as-synthesized  $\text{TiO}_2/\text{SiO}_2$  nanocomposites via a charge transfer process from the dye to the semiconductor [26]. Another contributing factor was the ability of these acquired charge carriers to migrate without much interaction amongst them [26]. The possibility of tunneling of charge carriers through the potential barrier

was also contributed towards better conductivity [27].

The photo conductivity plots of as synthesized and  $1 \times 10^{-5}$  M,  $2 \times 10^{-5}$  M,  $3 \times 10^{-5}$  M,  $4 \times 10^{-5}$  M,  $5 \times 10^{-5}$  M Safranin O dye-sensitized  $\text{TiO}_2/\text{SiO}_2$  nanocomposites with applied electric field was shown in fig. 15, a similar trend as in the dark current is seen. From the graph, it was evident that the photo current density values of the Safranin O dye-sensitized  $\text{TiO}_2/\text{SiO}_2$  nanocomposites increases with increase of dye concentration. It was observed that the photo current densities were higher than the dark current densities in all the cases. The variation of photocurrent with dye concentration for the fixed field of 200V/cm, 450V/cm and 600V/cm was shown in fig. 16. From the graph, it was observed that for the highest concentration of dye ( $5 \times 10^{-5}$  M), the photo current density increased in an order of 75 in comparison with that of  $\text{TiO}_2/\text{SiO}_2$  nanocomposites. For example, for a fixed field of 450 V/cm, the photo current density value of as-synthesized  $\text{TiO}_2/\text{SiO}_2$  nanocomposites was 0.01341 mA, whereas the photo current value of  $5 \times 10^{-5}$  M Safranin O dye-sensitized  $\text{TiO}_2/\text{SiO}_2$  nanocomposites was 1.0122 mA. The remarkable increase of photocurrent densities in the case of Safranin O dye-sensitized  $\text{TiO}_2/\text{SiO}_2$  nanocomposites was attributed to the presence of Safranin O dye in the composite which improves the spectral response of the  $\text{TiO}_2/\text{SiO}_2$  nanocomposites in the visible region. The threshold of light absorption generally corresponds to the excitation of an electron from valance band to conduction band [28, 29]. In the case of as-synthesized  $\text{TiO}_2/\text{SiO}_2$  nanocomposites, since it was photo-inactive in visible light, no significant increase in photocurrent was observed, whereas in the case of Safranin O dye-sensitized  $\text{TiO}_2/\text{SiO}_2$  nanocomposites, the photoactive Safranin O dye molecules were capable of absorbing photons of visible light and were excited to higher energy levels from where the electrons were transferred to conduction band of  $\text{TiO}_2/\text{SiO}_2$  nanocomposites and hence increase the free charge carrier concentration of the composite and in turn its photocurrent. Fig. 17 showed the difference in dark and photo current densities vs amount of dye adsorbed by  $\text{TiO}_2/\text{SiO}_2$  nanocomposites. From the graph, it was found that the difference in dark and photocurrent density increased linearly with increase of dye concentration. The Safranin O

dye has thus made the  $\text{TiO}_2/\text{SiO}_2$  nanocomposites photosensitive to the visible light.

## II. CONCLUSION

The binary system of  $\text{TiO}_2/\text{SiO}_2$  nanocomposites were synthesized by modified sol-gel method. XRD results confirms the formation of Ti-O-Si linkages in  $\text{TiO}_2/\text{SiO}_2$  nanocomposites, also revealed the presence of prominent peaks due to  $\text{TiO}_2/\text{SiO}_2$  nanocomposites and complete absence of peaks due to Safranin O dye due to the dye was physically adsorbed into the pores of the nanocomposites. FTIR confirmed the formation of Ti-O-Si linkages in  $\text{TiO}_2/\text{SiO}_2$  nanocomposites. Using Tauc Plot, the band gaps were calculated for all the dye-sensitized  $\text{TiO}_2/\text{SiO}_2$  nanocomposites. There was no change in the band gap with the increase of concentration of the dye solution. Field dependent dark and photoconductivity of Safranin O dye-sensitized  $\text{TiO}_2/\text{SiO}_2$  nanocomposites showed remarkable increase of photocurrent densities which could be attributed to the presence of Safranin O dye in the  $\text{TiO}_2/\text{SiO}_2$  nanocomposites which facilitates the onset of a charge transfer process wherein a photon absorbed by a dye molecule gives rise to electron injection into the conduction band of  $\text{TiO}_2$  nanostructures. The Safranin O dye has thus made the  $\text{TiO}_2/\text{SiO}_2$  nanocomposites photosensitive to the visible light. Thus Safranin O sensitized  $\text{TiO}_2/\text{SiO}_2$  nanocomposite will be a potential candidate for the construction of dye-sensitized solar cells

## REFERENCES

- Hagfeldt A, Gratzel, M Molecularphotovoltaics, Acc. Chem. Res. 33 (2000) 269-277.
- Klein S, Thorimbert S, W.F. Maier, Amorphous Microporous Titania-Silica Mixed Oxides: Preparation, Characterization, and Catalytic Redox Properties, J. Catal. 163 (1996) 476-488.
- R. Mariscal, M. López-Granados, J.L.G. Fierro, J.L. Sotelo, C. Martos, R. van Grieken Morphology and Surface Properties of Titania-Silica Hydrophobic Xerogels, Langmuir 16 (2000) 9460-9467.
- Frailé J. M, García J. I, Mayoral J. A, Vispe E, Catalytic sites in silica-supported titanium catalysts: silsesquioxane complexes as models, J. Catal. 233 (2005) 90-99.
- Martin A. Green, Keith Emery, Yoshihiro Hishikawa, Wilhelm Warta Solar cell efficiency tables, photovolt. res. Appl. 19 (2011) 84-92.
- Arun Kumar D, Francis P. Xavier, MerlineShyla J, Natural dye sensitization of  $\text{TiO}_2$  thin films using Lawsonia dye extracted from LawsoniaInermis for solar cell applications, Archives of Applied Science Research 4 5 (2012) 2122-2132.
- PlinioInnocenzi, Alessandro Martucci, Massimo Guglielmi, Andrea Bearzotti, Enrico TraversaElectrical and structural characterization of mesoporous silica thin films as humidity sensors 76 1-3 (2001) 299-303.
- Aguado J, Grieken R V, Munoz M.J.L, Marugan J, Comprehensive study of the synthesis characterization and activity of  $\text{TiO}_2$  and mixed  $\text{TiO}_2/\text{SiO}_2$  photo catalyst. Applied Catalysis A: General. 312 (2006) 202-212
- Anders Hagfeldt, BengtDidriksson, Tommy Palmqvist, Henrik Lindstrom, Sven Sodergren, HåkanRensmo, Sten-Eric Lindquist, Verification of high efficiencies for the Gratzel-cell. A 7% efficient solar cell based on dye-sensitized colloidal  $\text{TiO}_2$  films, Solar Energy Materials and Solar Cells 31 4 (1994) 481-488.
- Ponniah D, Xavier F, Electrical and electroreflectance studies on ortho-chloranil-doped polyanilinePhysica B 392 1-2 (2007) 20-28
- Arun Kumar K, Prakash SM, Low cost removal of Basic dye from aqueous solution using silk cotton hull, Journal of Environmental Research and Development 3 (2009) 728-734.
- Subba Reddy Y, Jeseentharani V, Jayakumar C, Nagaraja KS, Jeyaraj B Adsorptive removal of malachite green (oxalate) by low cost adsorbant, Journal of Environmental Research and Development 7 (2012) 275-284.
- Zhou Lijun, Shanshan Yan, BaozhuTian, Jinlong Zhang, Masakazu Anpo, Preparation of  $\text{TiO}_2\text{-SiO}_2$  film with high photocatalytic activity on PET substrate, Materials Letters 60 (2006) 396-399.
- KyeongYoul Jung, Seung Bin Park, Photoactivity of  $\text{SiO}_2/\text{TiO}_2$  and  $\text{ZrO}_2/\text{TiO}_2$  mixed oxides prepared by sol-gel method, Materials letter 58 (2004) 2897-2900.
- Li-Lan Yang, Yi-Sheng Lai, Chen JS, Compositional tailored sol-gel  $\text{SiO}_2\text{-TiO}_2$  thin films: crystallization, chemical bonding configuration and optical properties, Journal of Materials Research 20 (2005) 3141-3149.
- Arun Kumar D, MerlineShyla J, Francis P. Xavier, Synthesis and characterization of  $\text{TiO}_2/\text{SiO}_2$  nanocomposites for solar cell applications, Applied nanosciences 2 (2012) 429-436.
- Yin Zhao, Chunzhong Li, Xiuhong Liu, FengGu, Haibo Jiang, Wei Shao, Ling Zhang, Ying He Synthesis and optical properties of  $\text{TiO}_2$  nanoparticles, Materials Letter 61 (2007) 79-83.
- J Mohan, Organic Spectroscopy Principles and Applications, Narosha Publishing House Pvt. Ltd, 2<sup>nd</sup>edn. New Delhi, 2009, pp 28-95.
- Aziz RadhiyanAbd, SopyanIis, Synthesis of  $\text{TiO}_2\text{-SiO}_2$  powder and thin film photocatalysts of sol-gel method, International Journal of Chemistry 48 (2009) 951-957.
- XiaoyiShen, YuchunZhai, Yang Sun, HuiminGu, Preparation of monodisperse spherical  $\text{SiO}_2$  by microwave hydro-thermal method and kinetics of dehydrated hydroxyl, J Mater Sci Technol. 26 (2010) 711-714.
- MerlineShyla J, Electro-optical characterization of titanium dioxide-organic dye composites and fabrication of dye-sensitized solar cell using sol-gel coated  $\text{TiO}_2$  electrodes, Ph.D thesis, University of Madras, Chennai, 2005, pp. 196.
- Marie-Isabella Baraton, Nano- $\text{TiO}_2$  for solar cells and photocatalytic water splitting: scientific and technological challenges for commercialization, The open Nanoscience Journal 5 (2011) 64-77.
- Brian O'regan, Michael Grätzel, A low-cost, high-efficiency solar cell based on dye-sensitized colloidal  $\text{TiO}_2$  films, Nature 353 (1991) 737 - 740.
- Dhar S, Chakrabarti S Electroless, Ni plating on n and p-type porous silicon Si for ohmic and rectifying contacts, Semicond. Sci. Technol. 11 (1996) 1231-1234.
- Arun Kumar D, Francis P. Xavier, MerlineShyla J, Investigations on the variation of conductivity and photoconductivity of  $\text{CuO}$  thin films as a function of layers of coating, Archives of Applied Science Research 4 5 (2012) 2174-2183.
- Simon J, Andre JJ Molecular Semiconductors: Photoelectrical properties and solar cells, Springer-Verlag, Germany, 1985, pp. 6.
- Ponniah JD, Electrical conductivity and Spectral investigations of pure and doped polyaniline complexes, Ph.D thesis, University of Madras, Chennai, 2005, pp. 27.
- Xavier FP, Optical and Transport properties of Phthalocyanine and related compounds, UMI, Ann Arbor, 1993, pp. 48.
- Arun Kumar D, Alex Xavier J, MerlineShyla J, Francis P. Xavier, Synthesis and structural, optical and electrical properties of  $\text{TiO}_2/\text{SiO}_2$  nanocomposites, Journal of Materials Science 48 10 (2013) 3700-3707.